Bioresource Technology 267 (2018) 492–501

Contents lists available at ScienceDirect

Bioresource Technology

journal homepage: www.elsevier.com/locate/biortech

Assessment of transient effects of alternative nitrogen sources in continuous cultures of *Arthrospira* sp. using proteomic, modeling and biochemical tools

Neha Sachdeva[a], Giuseppe Giambarresi[a], Laurent Poughon[b], Juan Carlos Cabrera[c], Baptiste Leroy[a], Christophe Lasseur[d], Claude-Gilles Dussap[b], Ruddy Wattiez[a,*]

[a] Department of Proteomic and Microbiology, Research Institute of Biosciences, University of Mons, Mons 7000, Belgium
[b] Institut Pascal, Université Clermont Auvergne, CNRS, SIGMA Clermont, 4 avenue Blaise Pascal, Aubière 63178, France
[c] Biotechnology Unit, Materia Nova, Ghislenghien, Belgium
[d] European Space Agency, ESA/ESTEC, Noordwijk 2200, The Netherlands

GRAPHICAL ABSTRACT

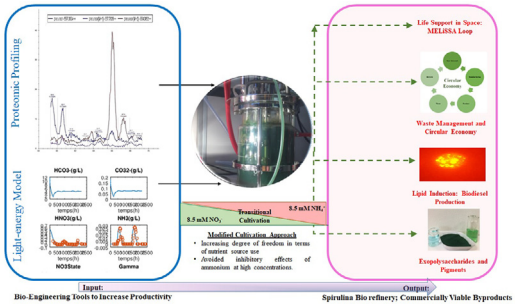

ARTICLE INFO

Keywords:
Arthrospira sp.
Alternative nitrogen source
Continuous cultivation
Proteomics
Light-energy transfer

ABSTRACT

The ability of cyanobacterium *Arthrospira* sp. to assimilate waste nitrogen sources (ammonium and urea) makes it an important candidate for wastewater management. The aim of this work was to evaluate a cultivation approach based on continuous-transitional-feeding regime (nitrate-ammonium-nitrate) in a photobioreactor to assess the effects of ammonium salts on *Arthrospira* sp. PCC 8005 metabolism. Using a comprehensive biochemical, proteomic and stoichiometric profiling of biomass, this study demonstrated that the proposed cultivation approach could increase the proteins and pigments yields by 20–30%, compared to the respective yields obtained from wild-type *Arthrospira* sp. strain A light-energy-transfer model was used to predict the biomass and oxygen productivities of *Arthrospira* sp. cultivated under transitional-feeding regime. 95 ± 2% match was observed between the experimental and simulated productivities. This study thus opened new avenues for use of ammonium rich wastewater for commercial production of high value pigments, biofuel and bioplastics using *Arthrospira* sp.

1. Introduction

The genetic robustness of cyanobacteria *Arthrospira* sp. and their versatility to adapt to a wide range of environmental conditions (pH, temperature, nitrogen sources, etc.) have increased their popularity with therapeutic, food, nutraceutical, waste water management, biofuel and various other commercial sectors (Zhou et al., 2017; Smetana et al., 2017; Shirazi et al., 2017; Jiang et al., 2015; Leema et al., 2010;

* Corresponding author at: Department of Proteomics and Microbiology, 20, Place du Parc, University of Mons, Mons 7000, Belgium.
E-mail address: Ruddy.Wattiez@umons.ac.be (R. Wattiez).

https://doi.org/10.1016/j.biortech.2018.07.062
Received 4 June 2018; Received in revised form 11 July 2018; Accepted 12 July 2018

Spolaore et al., 2006). Due to the wide range of applications, the global Spirulina (*Arthrospira* sp.) market is expected to reach the value of USD 1.8 million by the year 2026 (Persistence Market Research, 2017).

Though sodium nitrate ($NaNO_3$) is the mostly commonly used nitrogen (N hereafter) source for commercial cultivation of *Arthrospira* sp., the use of low-cost alternative N sources such as ammonium salts (NH_4^+ hereafter) could increase the economic viability of *Arthrospira* sp. production (Carvalho et al., 2004). NH_4^+ salts are not only cost effective but also metabolically preferred N sources for cyanobacterial cultivation (Rodrigues et al., 2010; Carvalho et al., 2004). Furthermore, with the depletion of fresh water resources and the burning issue of waste water management (rich in $NH_4)^+$, exploring the potential of using NH_4^+ rich waste water as the alternative N source for commercial *Arthrospira* sp. cultivation could aid in environmental remediation. Despite of these advantages, NH_4^+ salts are rarely used for cyanobacterial cultivation because of the lower biomass productivity and high pH associated inhibitory effects (Markou et al., 2016; Markou et al., 2014; Rodrigues et al., 2010; Carvalho et al., 2004).

The advantages associated with controlled feeding (fed batch or continuous cultivation) of nutrients to the photobioreactor (PBR) had been extensively reviewed in literature (Carvalho et al., 2004; Sassano et al., 2010; Markou, 2015). Interestingly, most of these studies conducted with the aim to evaluate the effect of different concentrations of NH_4^+ salts on productivities of photosynthetic cells (batch mode culture, pH ≥ 9.5), overlooked to factor in the effect of high pH on the NH_4^+/ammonia (NH_3) equilibrium (pKa = 9.25, temperature range 25–30 °C) in the cyanobacterial cultures. Sassano et al. (2010) conducted a study to evaluate the effect of different concentrations of NH_4Cl (vs KNO_3) on concentration and composition of *Arthrospira* sp. biomass, under fed-batch conditions (no pH control). The study reported decreased biomass productivities at NH_4Cl concentration > 5.0 mM. Since the pH was not controlled in this study, the lower productivities could have been the result of N starvation in the culture caused due to the loss (≥80%, pH > 9.2) of NH_4^+ ions as NH_3 (Collos and Harrison, 2014). Similar trends were reported by Deschoenmaeker et al. (2017) in their batch study, wherein the *Arthrospira* sp. fed with 6.0 mM NH_4^+ exhibited higher N uptake rates than the cells fed with 6.0 mM NO_3^-, potentially due to the high pH induced loss of NH_4^+ as NH_3.

At pH > 9.25 (temperature 25–30 °C), > 80% of NH_4^+ ions have been reported to be lost (gas-off) as gaseous NH_3 (Collos and Harrison, 2014). High NH_3 concentration had been further reported to have inhibitory effect on photosynthetic machinery of cells. Dai et al. (2008) investigated the effects of high NH_3 concentrations on Photosystem PSII of cyanobacterial cells and reported that NH_3 inhibits PSII activity by changing the photochemistry of oxygen evolving complex (OEC). Being a structural analog of water molecule, NH_3 can easily attach to oxidized OEC (see Supplementary data) and hence reduce the overall photosynthetic activity of cells. Dai et al. (2008) quantified this effect in terms of fluorescence (Fv/Fm) which was seen to decrease under high NH_3 concentrations. Markou et al. (2016) reported that gaseous NH_3 also inhibits the PSI activity, by damaging the reaction centers (RC) of thylakoid membrane. Since these RCs are the main sites for energy efflux and ATP generation, any damage caused to RCs changes photochemistry of the cells. Thus in summary, the prevalence of high pH in cyanobacterial cultures could lead to: (1) loss of NH_4^+ ions to gaseous NH_3, leading to the onset of nutrient starvation; (2) presence of dissolved NH_3 concentrations in the liquid phase, leading to metabolic inhibitions.

Arthrospira sp. have developed robust regulatory pathways for N metabolism (see Supplementary data). The exogenous N sources are sequestered intracellularly with the help of membrane transporters and are metabolized to simpler NH_4^+ form before being incorporated into GOGAT pathway. These chemical reactions are catalyzed by enzymes and are regulated by transcription operons (Deschoenmaeker et al., 2017). The N source used for *Arthrospira* sp. cultivation, thus has a significant impact on the metabolic and proteomic profile of the cells. Most of the previous proteomic studies on *Arthrospira* sp. had been limited to the use of NO_3^- salts. Deschoenmaeker et al. (2017) investigated the effect of N source transition (NO_3^- to NH_4^+, concentration 28 mM) on the proteomic profile of *Arthrospira* sp. The authors reported lower abundance of cyanophycin (N reserve compound) related proteins and higher abundance of N stress (depletion) related proteins under NH_4^+ regime.

The versatility of *Arthrospira* sp. to assimilate both organic (urea, glutamate, etc.) and inorganic (NH_4^+, nitrate) N sources, had earned this oxygenic cyanobacterium an important place in the field of life support in space (LSS) (Cornet et al., 1995). European Space Agency (ESA) through its MELiSSA (Micro Ecological Life Support System Alternative) project, aims to harness the oxygenic and waste recycling potential of *Arthrospira* sp. PCC 8005 (*Arthrospira* sp. henceforth) for production of edible biomass and oxygen (O2) for manned space missions. One of the main objectives of the MELiSSA loop is to improve the closure and simplicity of the loop, by bypassing the oxidation process (NH_4^+ to NO_3^-) and use the crew waste (urea, NH_4^+) as the N sources for *Arthrospira* sp. cultivation.

The present study aimed to evaluate the effect of transition between the two N sources (NH_4^+ and NO_3^- salts) and variable cultivation parameters (N source transition, N concentration 8.5 mM, pH 8.5 and temperature 36 °C) on O_2 productivity, stoichiometric yields, metabolic, proteomic, biochemical profile of *Arthrospira* sp. biomass. The biochemical and metabolic results were used to upgrade the light-energy transfer model (Cornet and Dussap, 2009) in order to facilitate accurate prediction of cyanobacterial growth and productivities in presence of two transiting N sources. This study thus made the pioneering attempt to develop a knowledge model and evaluate the impact of different N sources on the biochemical profile of the *Arthrospira* sp. The novelty of the study lies in the comprehensive profiling of *Arthrospira* sp. using stoichiometric, mathematical, biochemical, metabolic and proteomic tools. This study, thus, opens new avenues for the use of fluctuating stream of (waste) N sources for commercial production of photosynthetic microorganisms.

2. Materials and methods

2.1. Cyanobacterial strain cultivation, photo-bioreactor setup and growth profile

The stock culture of *Arthrospira* sp. strain PCC 8005 was photoautotrophically maintained in 250 mL Erlenmeyer flasks in Cogne Modified Zarrouk medium (Cogne et al., 2003) at 30 °C (pH 8.5, 8.5 mM $NaNO_3$) on rotary shaker (140 rpm) under continuous illumination of 60 μmol photons $m^{-2} s^{-1}$. Each liter of Cogne Modified Zarrouk medium contained 1.0 g of NaCl, 0.03 g of $CaCl_2$, 1.0 g of K_2SO_4, 0.08 g of $MgSO_4 \cdot 7H_2O$, 0.5 g of K_2HPO_4, 10.5 g of $NaHCO_3$, 7.6 g of Na_2CO_3, 0.08 g of EDTA, 0.01 g of $FeSO_4 \cdot 7H_2O$, and 1 mL per liter of the trace element solution containing (per liter) 0.23 g of $MnCl_2 \cdot 4H_2O$, 0.11*g* of $ZnSO_4 \cdot 7H_2O$ and 0.03 g of $CuSO_4 \cdot 5H_2O$.

A radially illuminated 2.0 L cylindrical double jacketed (Biostat®, Sartorius AG, Germany) PBR was used for the cultivation of photoautotrophic cultures (both batch and continuous mode) of cyanobacteria (see Supplementary data). Incident flux of 300 ± 50 μmol photon/m^2/s (Li-193SA; Li-Cor BioSciences, USA) was maintained using halogen lamps (Philips, 20 W, 12 V) and the agitation of 150 rpm was achieved with Rushton turbine. The pH (Mettler Toledo, InPro 3250) was automatically maintained at 8.5 with HCl (0.5 N) and NaOH (1.0 N). Turbidostatic regime under the continuous run was maintained with a dilution rate of 0.2 per day using Cogne Modified Zarrouk medium (8.5 mM $NaNO_3$ or NH_4Cl, pH 8.5). The PBR was continuously purged with 99.9% pure nitrogen gas at flow rate of 50 mL/min. Culture samples were collected every 24 h under axenic conditions and the biomass was recovered on filter (0.2 μm Sartorius

AG, Germany). The filtered biomass was washed thrice with distilled water, lyophilised and stored at −20 °C until further use for biochemical and proteomic analyses. Optical density (OD_{750}) of the harvested samples was measured in a spectrophotometer (HELIOS-ZETA UV–VIS, Thermo Scientific) at 750 nm, to rule out any chlorophyll interference (Chioccioli et al., 2014). The sedimentation index (SI) was used to monitor the stress profile of cyanobacterial cells as described by Deschoenmaeker et al. (2014).

2.2. Biomass and oxygen productivity

Dry cell weight (DCW) was determined from the filtered and dried biomass. The biomass productivity (g/L/day) was calculated by factoring in the dilution rate and biomass concentration (DCW, g/L) at the time the sampling as follows:

$$Biomass\ \ productivity\ \ (\mathrm{g/L/day}) = DCW\ \ (g/L) * dilution\ \ rate \tag{1}$$

The O_2 mole fraction (Analox Gas Analyser 9212) and gas flow rate (Brooks Instruments; GT1355 Sho-Rate G) were measured at the outlet of the PBR (standard temperature- pressure conditions) and were used to calculate the O_2 productivity (mg/L/h) and yield as follows:

$$\mathrm{O2}\ \ productivity\ \ (\mathrm{g/L/day}) = c\frac{Outlet\ \ Gas\ \ Flowrate\ \ (\mathrm{mol/h}) * \mathrm{Outlet\ \ mol\ \ fraction\ \ of}\ \ O_2(\%)}{Total\ \ reactor\ \ volume\ \ (L)} \tag{2}$$

where c is the conversion factor; c = 7.68 = 32 (*Molecular weight of* O_2) × 24 (h)/100

$$\mathrm{O2}\ \ yield\ \ (g/g\ \ biomass) = \frac{O2\ \ productivity}{Biomass\ \ productivity} \tag{3}$$

2.3. Biochemical analysis

The cyanophycin (CP) content in the biomass was estimated spectrophotometrically by the method described by Allen et al. (2005), using arginine as the standard. The Chlorophyll *a* (Chl*a*) and Chlorophyll *b* (Chl*b*) contents were quantified by the spectrophotometric assay described by Sesták (1971). The total phycobiliprotein content, reported as sum of C-Phycocyanin (C-PC) and Allophycocyanin (APC); was estimated by the method reported by Patel et al. (2006). Total lipid, total protein, exopolysaccharide (EPS) and uronic acid (UA) content were quantified spectrophotometrically as described by Deschoenmaeker et al. (2017). The residual NH_4^+ and NO_3^- ion concentrations in the culture were quantified by spectrophotometric assays (HELIOS-ZETA UV–VIS, Thermo Scientific) described by Ivančič and Degobbis (1984) and Sachdeva et al. (2016a), respectively. The method based on the principle of pyrolysis was used for the estimation of elemental composition (CHON content) in the lyophilised biomass (Flash 200 Elemental Analyser, Thermo Scientific™).

2.4. Proteomic analysis

The lyophilised biomass samples were processed for the proteomic analysis, as described by Deschoenmaeker et al. (2017). The raw MS/MS spectral data were analysed using ProteinPilot (version 5) against the *Arthrospira* sp. PCC 8005 protein database. Protein quantification was carried out by PeakView software (version 2.1.0.11041, AB Sciex, USA) based on precursors XIC (mass tolerance 10 ppm, RT tolerance 3 min). The relative abundance (fold change) of peptides was calculated and analysed for statistical significance using Software MarkerView (version 1.2.1, AB Sciex, USA). For quantification purposes only the proteins identified with at least two peptides, exhibiting 50% fold change (i.e., fold change either ≥1.5 or ≤0.66) and characterised by a $p\ value < 0.05$ were considered to be differentially regulated.

2.5. Stoichiometric and kinetics based knowledge modelling

The Photosim model (Cornet and Dussap, 2009; Cornet et al., 1995; Cornet et al., 1992) was developed with the following assumptions: 1) PBR was treated as continuous stirred-tank reactor (CSTR) and 2) the photosynthetic reaction was only considered to be limited by light transfer and not by other cultivation parameters (nutrients, pH, temperature, etc.). Based on these assumptions the original Photosim Model (Cornet and Dussap, 2009) was calibrated and validated under nutrient (N and light) replete conditions, with NO_3^- as the N source (28 mM, pH 9.5). The model was robust enough to be used for predicting the growth and productivities for different cultivation conditions (light, temperature, N-NO_3^- concentration, pH, etc.) and PBR geometries. The present study tested the validity of the model, (using the mathematical and stoichiometric equations of the original model) for the prediction of residual NO_3^-, NH_4^+ and O_2 concentrations in the PBR, under different (than original model) cultivation conditions (pH, temperature, light intensity, N concentration, etc.). All mathematical simulations for the model were performed in Octave (version 4.2.1). The mathematical parameters and equations were adapted from original Photosim model (Cornet and Dussap, 2009).

2.6. Statistical analyses

Samples for biochemical and proteomic analysis were chosen from timepoints corresponding to the days wherein the PBR was entirely under an individual N source. GraphPad Prism (version 6.0, GraphPad Sofftware, USA) was used for graphical interpretation of biochemical data wherein the results were represented as standard error mean of three replicates.

3. Results and discussions

3.1. System performance

8.5 mM feeding concentration was chosen on the basis of the results obtained in the previous N transitional study (28 mM feeding concentration, pH 9.5) by the authors (Deschoenmaeker et al., 2017), wherein *Arthrospira* sp. was found to assimilate a maximum of 12 mM NH_4^+. The PBR was operated at pH 8.5 to reduce N losses. The PBR was initially started under batch mode (Day 0–8) and no N source was changed during this period. Therefore, the biomass from this phase was not used for biochemical, metabolic and proteomic analysis. Continuous mode (NO_3^- 8.5 mM, pH 8.5, temperature 36 °C) was turned on Day 9 (D9) after reaching an optical density (OD_{750nm}) of 1.1 ± 0.2 (Fig. 1a). Four transitions (Table 1) were performed between $NaNO_3$ (NO_3^- hereafter) and NH_4Cl (NH_4^+ hereafter) (8.5 mM each) on D19 (to NH_4^+), D35 (to NO_3^-), D61 (to NH_4^+) and D75 (to NO_3^-), respectively. Biomass was harvested under the respective N regimes of continuous run and analysed to evaluate the effect of N regime and transition on the biochemical, metabolic and proteomic profile of *Arthrospira* sp. The run lasted for 90 days and significant increase in cell-clumping and biofilm secretion was observed towards the second half (post D40) of the run.

3.2. Effect of nitrogen source and transition on growth profile and nitrogen assimilation

OD_{750nm} exponentially increased till D8, while the PBR was running under batch mode. Once the PBR was put on the continuous mode (D9), a slight decrease was observed in OD_{750nm} following the first few days of the start of continuous mode (Day 9-Day 14; Fig. 1a). This slight decrease in the OD_{750nm} between Day 9 and Day 14, was attributed to two factors; 1) cell dilution and acclimatization of the cells to the transition from batch to continuous mode and/or 2) the onset of N deplete conditions caused due to N exhaustion (as evident from the

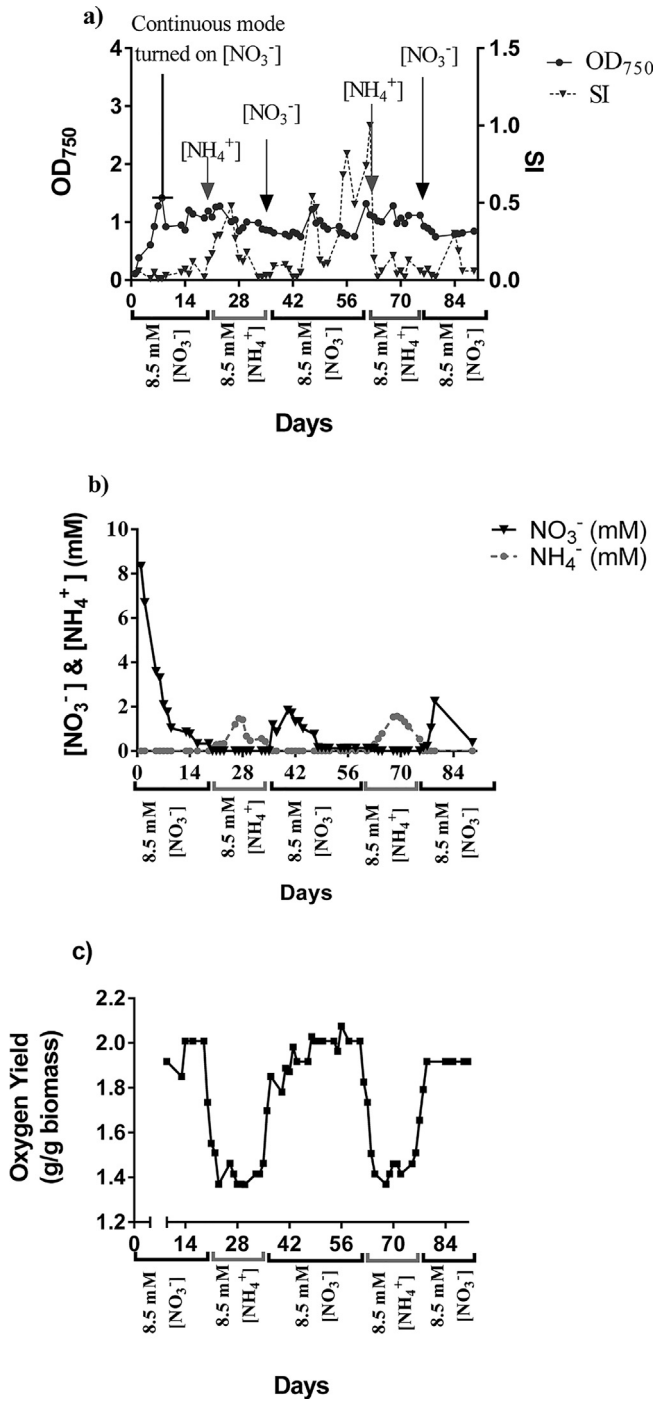

Fig. 1. Effect of nitrogen transition and source ($NaNO_3$ or NH_4Cl) on a) Optical Density (OD_{750nm}) and sedimentation index (SI), (b) nitrogen assimilation profile (residual $NaNO_3$ and NH_4Cl, in mM) and (c) oxygen yield (gO_2/g biomass) of *Arthrospira* sp. PCC 8005, cultivated in continuous PBR under controlled conditions of 8.5 mM total nitrogen, pH 8.5 and 36 °C.

total N concentration in PBR falling below 1.0 mM between D9 and D19; Fig. 1b) in the PBR. Since the increase in sedimentation index (SI) is an important marker of N starvation in the cyanobacterial cells (Depraetere et al., 2015), the increase in SI observed between D9 and D19 (Fig. 1a) further indicated at prevalence of cellular stress, potentially due to the onset of N starved conditions in the PBR.

First transition (to NH_4^+, D19) was performed, once the cells had adjusted to the new feeding regime and cells had reached a steady OD_{750nm} of 1.1 ± 0.2. A slight increase in the OD_{750nm} was observed following the first few days (D20 to D27) of NH_4^+ transition (Fig. 1a) potentially due to the influx of NH_4^+ ions in the culture vessel. The OD_{750nm} was seen to fall again (Fig. 1a) with the decrease in NH_4^+ content in PBR (Fig. 1b). Even though fresh feed was added continuously, the low N concentration in PBR coupled with dilution rate of 0.2 day^{-1} was not adequate to sustain the high cell density, which led to the onset of N starved conditions within a few days of the transition. Similar profiles in terms of growth, N assimilation and SI were observed for the subsequent transitions. To verify that no NH_4^+ was lost due to gassing off as NH_3, gaseous NH_3 was measured (Gastec NH_3 Detector Tubes, Japan) at PBR outlet. Absence of gaseous NH_3 at the outlet indicated that all of the NH_4^+ fed into the PBR was being fully assimilated by the cyanobacterial cells and no significant gassing off occurred at controlled pH of 8.5. In other words at pH 8.5, the partial pressure of NH_3 (for the total residual NH_4^+ concentration) in the culture was always maintained below the threshold value (equilibrium), thus avoiding any inhibitory effects on cyanobacterial growth.

These preliminary results demonstrated that the cells could adapt to the new N regime and continue to grow in presence of NH_4^+ as the N source. It was also concluded that NH_4^+ could be effectively used as an additional/ alternative N source for *Arthrospira* sp. cultivation without any inhibitory effects (provided the pH is maintained below 8.5). These results also indicated that the use of alternative N sources could be explored for the sustainable terrestrial cultivation of *Arthrospira* sp. Furthermore, the potential of using NH_4^+ rich wastewater (Zhou et al., 2017; Jiang et al., 2015) for *Arthrospira* sp. cultivation could also help in reducing the dependence on fresh clean water for cyanobacterial cultivation.

3.3. Effect of nitrogen source and transition on biomass productivity and oxygen yield

The average biomass productivities of 0.52 g/L/day and 0.5 g/L/day were observed under the NO_3^- and NH_4^+ regimes, respectively (Table 1). The comparable biomass productivities under both N regimes further indicated that NH_4^+ could be effectively used as a cost effective alternative N source for the commercial *Arthrospira* sp. production.

The difference in the chemical composition of NO_3^- and NH_4^+ salts was seen to have a direct impact on O_2 yields and productivities of biomass. Based on this chemical difference, a variation was expected between the O_2 yield and productivity under the NH_4^+ and NO_3^- feeding regimes. Experimentally, an average O_2 yield of 1.9 gO_2/g biomass and O_2 productivity of 1.0 gO_2/L/day were observed under NO_3^- feeding regime (Table 1, Fig. 1c). On the other hand, average O_2 yield of 1.5 gO_2/g biomass and O_2 productivity of 0.7 gO_2/L/day were observed under NH_4^+ feeding regime. The respective 77% and 70% variation (experimental data) observed for the average O_2 yield and productivities between the two N sources was in line with the difference in their chemical content.

3.4. Effect of nitrogen source and transition on biochemical profile

An average of 15.4% lipid (as % of DCW) content (Table 1) was observed in the biomass harvested under NH_4^+ regime (D20-35 and D62-75) which was 13.5% higher than the average lipid content of 13.1% observed in biomass cultivated under NO_3^- regime (D9-D19, D36-D61 and D76-D90). These values were higher than the average lipid content of 6–10% (as % DCW) previously reported for *Arthrospira* sp. (Baunillo et al., 2012; Leema et al., 2010; Spolaore et al., 2006). The higher than usual lipid content quantified under present study conditions, further indicated that the PBR was operating under N starved conditions, which had been reported to increase fatty acid (lipid) content in photosynthetic cells (Sachdeva et al., 2016a).

The total exopolysaccharide content (as % of DCW) of the cyanobacterial biomass harvested under the two N regimes was reported as the sum of EPS and UA (Uronic Acid), quantified in the separated

Table 1
Effect of nitrogen source transition (8.5 mM, pH 8.5) on average biomass productivity, oxygen yield and biochemical profile of *Arthrospira* sp. PCC 8005 cultivated in continuous PBR*.

Day	NR	PB* (g/L/day)	YO_2* (g/g DCW)	PO_2* (g/L/day)	TL*Δ (%)	TP*Δ (%)	TPS*ΔΨ (%)	TChl* (mg/L)	C-PC* (g/L)	APC* (g/L)	CP* (g/L)
9–19	NO_3^-	0.52 ± 0.01	1.9 ± 0.4	1.0 ± 0.3	12.1 ± 2.1	50.5 ± 7.3	25.8 ± 5.9	120.0 ± 36.9	1.2 ± 0.1	0.7 ± 0.2	4.6 ± 0.5
20–35	NH_4^+	0.50 ± 0.03	1.5 ± 0.3	0.7 ± 0.1	15.2 ± 1.4	40.3 ± 6.3	39.8 ± 4.2	90.0 ± 26.6	0.9 ± 0.2	0.6 ± 0.1	1.4 ± 0.5
36–61	NO_3^-	0.52 ± 0.02	1.9 ± 0.5	1.0 ± 0.1	12.6 ± 0.8	49.8 ± 6.1	23.2 ± 7.0	110.0 ± 14.1	1.2 ± 0.1	0.7 ± 0.2	4.8 ± 0.7
62–75	NH_4^+	0.50 ± 0.03	1.5 ± 0.7	0.7 ± 0.1	15.6 ± 2.3	39.4 ± 5.7	42.8 ± 10.1	70.0 ± 17.7	0.5 ± 0.2	0.4 ± 0.1	1.6 ± 0.3
76–90	NO_3^-	0.52 ± 0.04	1.9 ± 0.6	1.0 ± 0.2	14.7 ± 3.7	48.2 ± 8.4	31.5 ± 4.7	80.0 ± 8.8	0.9 ± 0.2	0.5 ± 0.1	4.2 ± 0.6

NR: Nitrogen Regime; ***PB***: Biomass Productivity; ***PO_2***: Oxygen Productivity; ***YO_2***: Oxygen Yield; ***DCW***: Dry Cell Weight; ***TL***: Total Lipid; ***TP***: Total Protein; ***TPS***: Total Polysaccharide; ***TChl***: Total Chlorophyll as sum of *Chl*a and *Chl*b; ***C-PC***: C-Phycocyanin; ***APC***: Allophycocyanin, ***CP***: Cyanophycin.

* Values reported as an average (± standard deviation) of all the timepoints of the respective transitions/nitrogen regime.

Δ The values reported as the percentage of total dry cell weight (DCW) of biomass.

¥ Total polysaccharide (TPS) content reported as sum of Exopolysaccharide (EPS) and Uronic acid (UA) content, quantified in biomass and supernatant for the respective timepoints.

biomass (active biomass) and supernatant. The total exopolysaccharide content in the supernatant (released as exogenous glycogen due to nutrient stress induced cell lysis) was regarded as a passive biomass fraction. Consequently, an average of 41.3% total exopolysaccharide content was observed in the biomass (active and passive) cultivated using NH_4^+, compared to average 26.9% total exopolysaccharide content observed under NO_3^- regime (Table 1). Since the increased EPS and UA secretions are an important biological marker of cellular stress (Depraetere et al., 2015), these results along with the SI (Fig. 1a), further indicated that regardless of the N source used, the culture was constantly under N starvation. Recent studies on cyanobacterial exopolysaccharides had demonstrated the potential use of these polymers in synthesis of biodegradable plastics and medical prosthetics (Zeller et al., 2013; Bhatnagar et al., 2014). Therefore, this ability of *Arthrospira* sp. cells to secrete high concentrations of exogenous polysaccharides, could be harnessed for the production of environmentally friendly bioplastics and wound healing biomaterials.

Irrespective of the N source used, significant decrease was observed in the protein content of the biomass cultivated under present study conditions (Table 1). The cellular protein contents (as % of DCW) were found to be lower than the expected levels of 65–70%, previously reported for *Arthrospira* sp. (Spolaore et al., 2006). An average of 49.5% and 39.9% total protein content was quantified in the biomass cultivated under NO_3^- (D9-19; D36-61; D76-90) and NH_4^+ (D20-35; D62-75) regimes (Table 1). The lower than expected protein content in the cells could also be linked to the low cyanophycin (CP) content in the cells (Table 1). CP is an important N storage compound found in cyanobacterial cells (Oppermann-Sanio and Steinbüchel, 2002) and is thus an important biological marker to quantify endogenous N storage. On an average, the CP content was found be higher in the biomass fed with NO_3^- (vs NH_4^+). The relatively low protein content of the harvested biomass further indicated that irrespective of the N source used, the cells were constantly under N starved conditions.

The overall total pigment content of the biomass was found to be approximately 40 to 20% lower under NH_4^+ regime (vs NO_3^- regime). Briefly the total (average) chlorophyll content (reported as sum of Chl*a* and Chl*b*) of biomass cultivated under NH_4^+ regime (80 mg/L) was found to be 22.3% lower than the total chlorophyll content observed for the biomass cultivated with NO_3^- (103 mg/L) as N source (Table 1). Similarly, the C-Phycocyanin (C-PC) and Allophycocyanin (APC) content were found to be respectively higher by 36.61 and 25.39% under NO_3^- regime (vs NH_4^+ regime). The lower pigment content in the biomass cultivated with NH_4^+, could be linked to the lower activity of the Photosystem I (PS I) and Photosystem (PS II) under NH_4^+ regime (Xu et al., 2001). These results were in line with the lower O_2 yield under NH_4^+ regime and were further verified by the lower abundance of photosynthetic proteins in the biomass harvested under NH_4^+ regime (proteomic analysis; Section 3.6). Despite of the prevalence of N starved conditions, the average C-PC (0.71 g/L) and total chlorophyll (80 mg/L) values under NH_4^+ feeding conditions were considerably higher than the previously reported value of 0.35 g/L (C-PC) and 5.3 mg/L (Chlorophyll), reported for *Arthrospira* sp. cultivated with 28 mM $NaNO_3$ (Leema et al., 2010). This potential of obtaining higher pigment content using present cultivation approach could be explored for the profitable production of high value pigments using low cost (alternative) N sources.

3.5. Stoichiometric knowledge model

3.5.1. Model validation: elemental and compositional analysis of biomass

Modifications in the cultivation parameters (N source, N starvation, pH, temperature, etc.) had been shown to modify the compositional profile of the cells corresponding to differential proteins expression. This change could be a consequence of the adaptation of the intracellular behavior and of the main metabolic pathways to variable cultivation conditions, i.e., continuous or batch, N source, etc. N limitation had also been reported to increase the lipid content and lower the protein content of the photosynthetic cells (Sachdeva et al., 2016a, 2016b).

In terms of modeling, the original Photosim Model (Cornet and Dussap, 2009) was developed for *Arthrospira* sp. cultivated using NO_3^- (28 mM) as N source (pH 9.5, 30 °C). For these reference conditions, the original model relied on a stoichiometric approach based on a fixed elemental biomass composition ($CH_{1.57}O_{0.41}N_{0.17}$) and exopolysaccharide ($CH_{1.65}O_{0.95}$) content, the proportions of which were dependent on the incident light flux in the culture (Cornet and Dussap, 2009). Since cultivation parameters and N concentration were observed to modify the biochemical profile of the biomass, it became necessary to re-evaluate the elemental composition of the biomass cultivated under the present study conditions. For this purpose two batch runs (one each with 8.5 mM NH_4^+ and NO_3^-) were conducted under the controlled conditions of the PBR (pH 8.5, temperature 36 °C, 150 rpm). The biomass harvested under the two batch runs was used for calculating the elemental composition of the *Arthrospira* sp. cultivated under the modified cultivation parameters of the present study.

The elemental composition (Table 2) of the cyanobacterial cells for the original Photosim model was calculated on the basis of their total carbon (C) content (Cornet and Dussap, 2009). The elemental composition of the biomass harvested under the batch runs (this study) were found to be different from the elemental composition of the biomass obtained under the original reference conditions used for Photosim model, potentially due to variations in pH, N source and concentration (Table 2). At steady state, C-molar compositions of $CH_{1.811}O_{0.511}N_{0.152}$ and $CH_{1.807}O_{0.508}N_{0.175}$ were quantified for the biomass harvested under NH_4^+ and NO_3^- conditions, respectively (data not shown). After factoring in the metabolites released in the supernatant, the total biomass compositions and excreted metabolites, the following compositions: $CH_{1.58}O_{0.362}N_{0.156}$ and $CH_{1.56}O_{0.380}N_{0.183}$ were obtained for

Table 2
A comparative of biochemical and elemental composition of *Arthrospira* sp. PCC 8005 biomass cultivated under present conditions (pH 8.5, 36 °C, 8.5 mM total nitrogen as NH_4Cl or $NaNO_3$) vs the biomass cultivated with the parameters of Classical model.[ϕ]

N Source	% Complex Polysaccharide[¥,*,§]		% Protein[*]	% Lipid[*]	Elemental Composition
	% EPS	% UA			
[Δ]NH_4Cl	17.9	26.3	47.4	20.6	$CH_{1.58}O_{0.362}N_{0.156}$
[Δ]$NaNO_3$	12.6	10.0	53.1	12.2	$CH_{1.56}O_{0.380}N_{0.183}$
[ϕ] Photosim Model	25.5	–	48.1	9.6	$CH_{1.57}O_{0.459}N_{0.173}$

[Δ] Cultivated at pH 8.5, 8.5 mM N (NH_4Cl or $NaNO_3$), 36 °C.
[ϕ] Cultivated at pH 9.5, 28 mM $NaNO_3$, 30 °C (Cornet and Dussap 2009).
[*] Reported as % of biomass.
[¥] Value reported were as a sum of respective analyte quantified in lyophilised biomass (active biomass) and supernatant. The results were expressed as percentage of active biomass. For the calculation of stoichiometric equation only the polysaccharide content sticking to the biomass (active biomass) was taken into consideration and the polysaccharide content obtained in supernatant was regarded as passive biomass.

NH_4^+ and NO_3^- batch runs, respectively (Table 2). These values were consistent with the elemental and experimentally quantified macro-compound (proteins, lipids, UA, EPS) composition of the biomass (Table 2). Consequently, O_2 yields (gO_2/g biomass) of 1.63 and 2.06, respectively were obtained for NH_4^+ and NO_3^- batches, as per the following stoichiometric equations:

$$CO_2 + 0.156NH_3 + 0.556H_2O \longrightarrow CH_{1.58}O_{0.362}N_{0.156} + 1.097O_2$$

$$CO_2 + 0.183HNO_3 + 0.688H_2O \longrightarrow CH_{1.56}O_{0.380}N_{0.183} + 1.429O_2$$

Additionally, based on the elemental composition and steady state C-molar compositions of biomass ($CH_{1.811}O_{0.511}N_{0.152}$: NH_4^+ and $CH_{1.807}O_{0.508}N_{0.175}$: NO_3^-), comparable O_2 yields (gO_2/g biomass) of 1.4 and 1.9 were obtained for the NH_4^+ and NO_3^- batches, respectively. These values were totally consistent (95 ± 2% match) with the average experimental O_2 yields (gO_2/g biomass) of 1.5 (NH_4^+) and 1.9 (NO_3^-), observed for the respective N regimes of the continuous PBR run (Section 3.3, Table 1). Thus, effectively all three methods: (a) elemental composition based stoichiometric analysis of biomass, (b) stoichiometric analysis obtained from macro-compounds composition and (c) direct measurement of yields from gas balance on continuous cultures; returned comparable O_2 yields. The consistency between the simulated and experimental results further indicated that the suggested 'C-molar' based stoichiometric profiling of the biomass under the two N regimes were correct and robust enough to perform further predictions and simulations, provided that the variation in the cultivation parameters are taken into account.

N starvation was observed to cause significant variations in the total exopolysaccharide and lipid content of the biomass harvested from the batch runs. The protein content of biomass (under batch runs, 8.5 mM N) cultivated with NH_4^+ and NO_3^- as N sources, were respectively found to be 47.4% and 53.1% (of DCW). On the other hand, the total lipid content of biomass cultivated using NO_3^- and NH_4^+ were found to be 12.2 and 20.6% (of DCW), respectively as opposed to 9.6% observed under original reference conditions of 28 mM $NaNO_3$ (Table 2). It must be noted here that the protein content reported here for batch runs, was calculated as an average of the protein content of the biomass harvested for the first three days of the respective batch run. Since the N concentration during these first three days of the batch had not reached limiting levels (as opposed to the continuous run, Section 3.4) the relative protein content was thus found to be higher for the samples harvested under batch conditions.

The higher than usual exogenous polysaccharide content (EPS and UA) in biomass using NH_4^+ as N source (Table 2) were in line with the results previously reported by Deschoenmaeker et al. (2017), wherein N starvation was seen to increase the secretion of exogenous polysaccharides. However, for the purpose of the calculation of the stoichiometric profile of the biomass, only the exopolysaccharide content in the (active) biomass and not supernatant (passive biomass) were taken into consideration.

Table 3
A comparative of the predictive modelling parameters of light energy transfer model used for calculation of productivities under present cultivation conditions vs Photosim Model.[ϕ]

Predictive Parameter	Notation	Photosim Model[ϕ]	Present study[Δ,*]
Mass absorption coefficient ($m^2\,kg^{-1}$)	Ea	162.00	300.00
Mass scattering coefficient ($m^2\,kg^{-1}$)	Es	640.00	1100.00
Maximum energetic yield	ρ_M	0.80	0.80
Mass Quantum Yield ($kg_x\,\mu mol_{hv}^{-1}$)	ϕ	1.85 e^{-9}	8.25 e^{-9}
Half saturation constant ($\mu mol\,m^2\,s^{-1}$)	*K*	90.00	20.00
Dark fraction of reactor	f_d	0	0
Reactor Illumination ($\mu mol\ photons\,m^2\,s^{-1}$)	F_0	30 to 1600	350
Specific illuminated area (m^{-1})	a_{light}	25.00	50.00

[Δ] Cultivated at pH 8.5, 8.5 mM nitrogen (NH_4Cl or $NaNO_3$), 36 °C.
[ϕ] Cultivated at pH 9.5, 28 mM $NaNO_3$, 30 °C (Cornet and Dussap 2009).
[*] Similar parameters used for both NH_4Cl and $NaNO_3$, no separate values calculated for NH_4Cl.

3.5.2. Validation of experimental yields using Photosim model

The predictive parameters of original Photosim model and simulation equations were derived on the basis of the stoichiometric profile of the cyanobacterial cells cultivated under N replete conditions (Cornet and Dussap, 2009). However, since the biochemical profile of the cyanobacterial cells (present study) was seen to change with the change in pH, N concentration and source, it was important to derive the new predictive parameters for the model simulation. The revised predictive parameters defined for model simulation for the present study conditions have been reported under Table 3.

The variations in the cultivation conditions (present study, continuous PBR run) were seen to impact the stoichiometric profile (Section 3.5.1) of the biomass (and hence the stoichiometric equations). It was necessary to test the robustness of the model in the context of present study (varying cultivation conditions of pH, N concentration and source). For this purpose, the first simulation (see Supplementary data) to predict the O_2 production rate and $NaNO_3$ and NH_4Cl concentrations in liquid phase, were performed with the stoichiometric equations corresponding to the reference conditions and predictive parameters of the original Photosim model (Cornet and Dussap, 2009). The simulation results, in terms of O_2 production rates obtained under NO_3^- and NH_4^+ feeding conditions were observed to vary by 79%, which were comparable to the 77% variation observed under experimental conditions (Table 1). However, deviations were observed between the fitting of the simulated and experimental values for residual NO_3^- and NH_4^+ concentrations (g/L) in the continuous run of the PBR (especially for NH_4^+). These deviations could be attributed to the variations in the stoichiometry and prediction parameters (original vs present conditions, Table 3), which were originally calculated on the basis of the elemental composition of the biomass cultivated with 28 mM $NaNO_3$. The deviations were more significant for the days when the PBR was undergoing a transition (change from one N source to other), potentially due to the changing kinetic, metabolic and stoichiometric profiles of the cells attempting to adapt to the new N source.

Therefore, in order to have a more accurate prediction, a new simulation was performed with the revised compositional (Table 2, Fig. 2) and predictive (Table 3) model parameters. With the revised

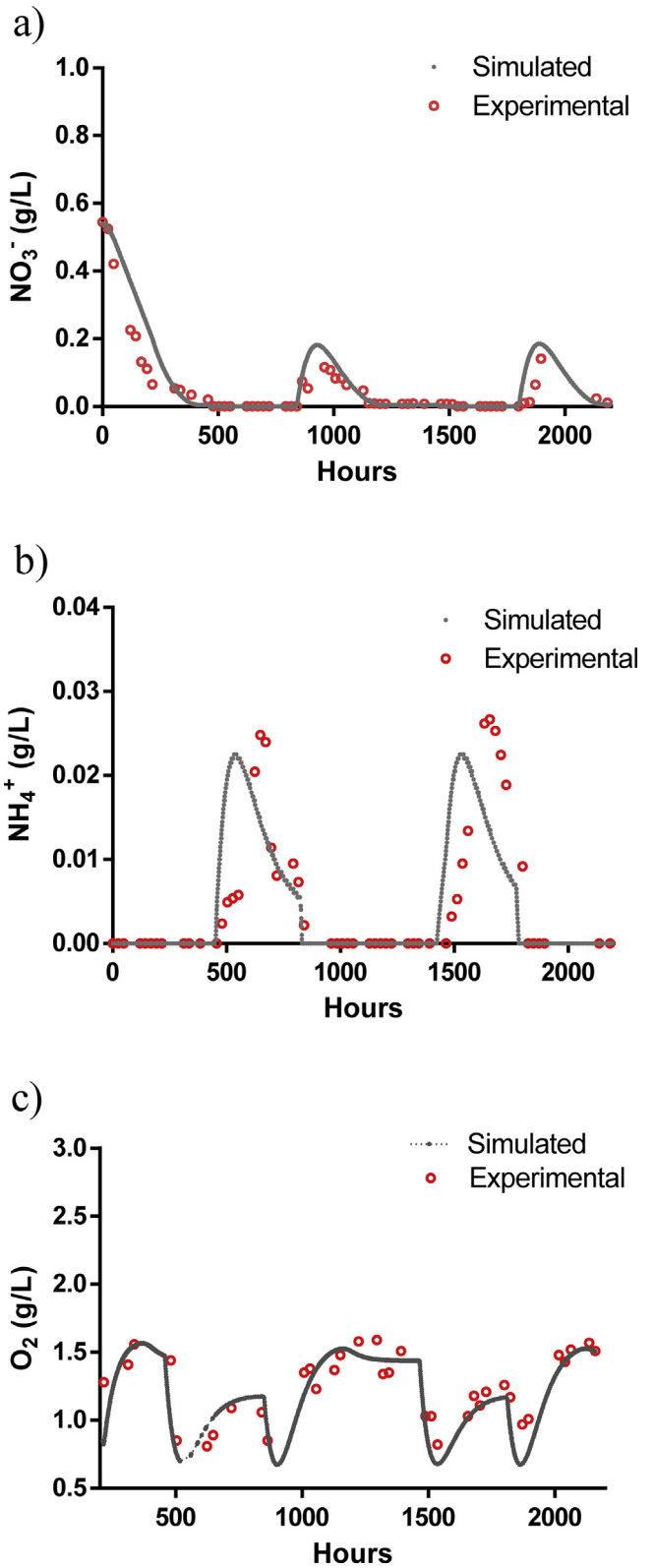

Fig. 2. A comparative of the experimental and simulated results of residual a) NO_3^- (g/L), (b) NH_4^+ (g/L) and (c) O_2 (g/L) concentrations in PBR, under continuous cultivation of *Arthrospira* sp. PCC 8005 (transition from $NaNO_3$ to NH_4Cl; 8.5 mM total nitrogen, pH 8.5, 36 °C). *Simulation performed with the revised predictive parameters in context of the stoichiometry of present cultivation conditions.*

stoichiometric equations and predictive model parameter, best fittings (experimental vs simulated values) were observed for NO_3^- (Fig. 2a) and O_2 (Fig. 2c) concentrations in the PBR, irrespective of the fact whether the PBR was fully working under individual N source or was under transition between the two N sources. However, for the NH_4^+ regime (Fig. 2b), accurate fittings (simulated vs experimental data) were only observed for the days wherein, a buildup (experimental) of the NH_4^+ was observed in the PBR. On the other hand, only 70–80% fitting was observed for the timepoints wherein the PBR was under transition between the two N sources. This misfit could be potentially attributed to the fact that prediction parameters (Table 3) were derived based on the quantum profile (used for calculation of predictive parameters) of the biomass cultivated using NO_3^- source. The change in the N source (and hence its stoichiometry) had a direct impact on the quantum (and hence metabolic profile: ATP, NADPH, etc.) of the biomass. Furthermore, these predictive parameters (quantum yield, light transfer coefficients, etc.) used for simulation were based on the light transfer, adsorption and scattering profile of the biomass. Due to the prevalence of acute N deplete conditions in the culture (specially under NH_4^+ feeding regime) a considerable amount of exopolysaccharides were exogenously secreted into the culture (as glycogen: passive biomass). The presence of high concentration of passive biomass in culture could have led to changes in the light transfer profile (light adsorption and scattering) of the biomass (not taken into account for the purpose of present study) and hence led to the 20–30% variation between the experimental and simulated results under NH_4^+ regime. Therefore, for future studies, it would be necessary to take into account the variation in the biomass size and type (cell aggregates, clumps, biofilm formation) caused due to the prevalence of N limitation conditions in the culture and re-calculate the prediction parameters accordingly for better and accurate predictions under N limiting conditions.

3.6. Proteomic analysis

The proteomic analysis was performed on the samples harvested under both N regimes to evaluate the effect of N source transition on *Arthrospira* sp. metabolism, with particular interest in proteins involved in N metabolism and photosynthetic activity of the cells. A total of 1515 proteins were subjected to Principal Component Analysis (PCA) to compare the relative abundance (as fold change) of the proteins under the two N regimes. The unsupervised PCA highlighted an unexpected trend by grouping of the samples more closely on the basis of the operational duration of PBR run, than based on N source (Fig. 3). Therefore, the proteomic data was submitted to statistical analyses under two subgroups: (a) the N source: *$NaNO_3$ on NH_4Cl* and (b) operational duration of PBR run: *late on early* (i.e., post D40 samples on pre D40 samples). The detailed results of the proteomic study could be found under the Supplementary data.

N source (*$NaNO_3$ on NH_4Cl*) was not seen to have a major effect on cyanobacterial proteomic profile. Of the 1309 proteins (out of 1515 total) quantified with at least two peptides, only 0.4% of these proteins was seen to be significantly impacted (p *value* < 0.05) by the change in N source (see Supplementary data). No statistically significant changes were observed in the proteins involved in C and N metabolism. This was contrary to the results observed by Deschoenmaeker et al. (2017) in their N transitional study (28 mM N, pH 9.5) wherein, N transition (NO_3^- to NH_4^+) was seen to exhibit significant impact of proteins related to N metabolism. However, a few photosynthetically relevant proteins like PS II related *psbY* and NADH cofactors (PS I related) *ndhJ*, *ndhA*, *NDC* were seen to have a respective 1.9, 3.9, 1.6 and 6.1 folds higher abundance under NO_3^- regime (Table 4). The lower abundance of proteins related to the photosynthetic machinery of the cells under

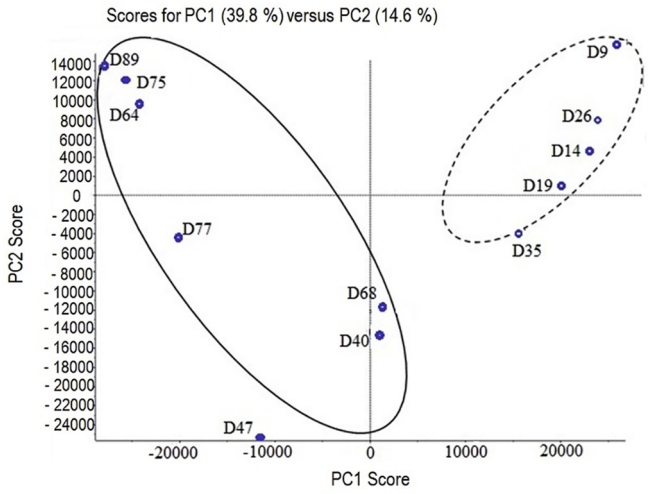

Fig. 3. Overview of Principle Component Analysis (PCA) of samples subjected to proteomic analysis using *ProteinPilot* Software. The unsupervised PCA (1515 proteins) clearly grouped samples on basis of operational duration of PBR run, with clear variation of 54.4% between PC1 vs PC2 scoring. The dotted circle represented the samples from the early phase (Pre D40) of the experiment while dark circle represented late phase (Post D40) samples. *Samples were named based on the day (D) of their harvesting.*

NH_4^+ regime was in line with the previous literature reports suggesting that due to its lower redox potential, NH_4^+ requires less energy for its assimilation (Markou et al., 2014).

N source was also seen to impact a few biologically relevant proteins, but the observed changes were not statistically significant. The higher abundance (≥1.5 fold change) of photosynthetic proteins (*psaE, psb27, psaA, petJ,* etc.) under NO_3^- regime indicated at better photosynthetic performance of cells under NO_3^- feeding, (Roose et al., 2007; Trebitsh and Danon, 2001) and effectively translated into higher O_2 yield and pigment content (Table 1). Furthermore, the lower abundance of CP linked proteins (*cph*A, *cph*B, etc.) under the NH_4^+ regime (see Supplementary data) could be corroborated with the biochemical data (Table 1), wherein lower CP accumulation was observed under NH_4^+ regime (vs NO_3^-). Overall, the N source based statistical analysis indicated that under N limited conditions (8.5 mM), the N source did not have major effect on the metabolic profile of *Arthrospira* sp. The absence of any statistically relevant effect of NH_4^+ on the metabolic profile of the cells under the present cultivation conditions further indicated that NH_4^+ can be used as an effective N source (in addition/ alternative to NO_3^-) for *Arthrospira* sp. cultivation without compromising on productivity.

On the other hand, the 'operational duration' of PBR run based statistical analysis (*late on early* or post D40 samples on pre D40) was seen to have significant impact on cyanobacterial proteome. Healthy (no stress) *Arthrospira* sp. cells are known to contain gas vesicles, which are responsible for their buoyancy and prevent cell sedimentation (Depraetere et al., 2015). Cellular stress is known to disrupt these gas vesicles, thus increasing the SI (Fig. 1a). The higher abundance of gas vesicle proteins (*gvp*) is thus an important cellular health marker in *Arthrospira* sp. cells. The lower abundance of *gvpC* and *gvpV* (0.07 and 0.59 folds, respectively) in the late phase (post D40) samples, indicated at higher cellular stress in late phase culture (Table 5). Similarly, proteins related to photosynthetic machinery (photosystem, pigments) were also seen to have lower abundance in the late phase culture (Table 5). The lower abundance of photosynthetically relevant proteins (PS I, APC and C-PC related, see Supplementary data) clearly indicated at reduced photosynthetic performance after prolonged operation of PBR. Briefly the proteins *cpc*B, *cpcC*2, *apc*C, *psa*D, *psa*B and *psa*L showed lower abundance by 0.01, 0.004, 0.12, 0.01, 0.18 and 0.04 folds, respectively under the late stage (post D40) samples when compared to early stage (pre D40) samples.

A few studies in the past had focused on the effect of 'culture run

Table 4
Effect of nitrogen regime ($NaNO_3$ on NH_4Cl) on the proteomic profile of *Arthrospira* sp. PCC 8005, cultivated in continuous PBR under transition of nitrogen regime *(p value < 0.05, number of peptides > 1 and fold change ≥ 1.5 or ≤ 0.66)*[*].

Protein Name	Annotation	Fold Change ($NaNO_3/NH_4Cl$)	Number of peptides	*p value*
ARTHROv5_60547|ndhJ (NAD(P)H-quinone oxidoreductase, subunit J)	*ndhJ*	1.9	10	$6.7\ e^{-3}$
ARTHROv5_61031|psbY (Photosystem II protein Y)	*psbY*	6.1	2	$1.5\ e^{-2}$
ARTHROv5_10689|ndhA (NADH: ubiquinone oxidoreductase, subunit H)	*ndhA*	3.9	3	$3.4\ e^{-2}$
ARTHROv5_30863|NDC (NADH dehydrogenase C1)	*NDC*	1.6	5	$3.9\ e^{-2}$

* Only statistically relevant (p value < 0.05, number of peptides > 1 and fold change ≥ 1.5 or ≤ 0.66) results reported here.

Table 5
Effect of operational duration of PBR run (late on early) on the proteomic profile of *Arthrospira* sp. PCC 8005, cultivated in continuous PBR under transition of nitrogen regime *(p value < 0.05, number of peptides > 1 and fold change ≥ 1.5 or ≤ 0.66).*[*]

Protein Name	Annotation	Fold Change (Late/ Early)[**]	Number of peptides	*p value*
Photosynthetic machinery (pigments, photosystems) related proteins				
ARTHROv5_11553|cpcB (C-phycocyanin beta subunit)	*cpcB*	0.01	278	$2.1\ e^{-6}$
ARTHROv5_11556|cpcC2 (Phycobilisome related protein)	*cpcC2*	$4.0\ e^{-3}$	48	$1.0\ e^{-3}$
ARTHROv5_10635|apcC (Allophycocyanin associated)	*apcC*	0.12	6	$1.3\ e^{-9}$
ARTHROv5_30080|psaD (PS I reaction center subunit II)	*psaD*	0.01	34	$1.7\ e^{-2}$
ARTHROv5_10985|psaB (PS I apoprotein A2)	*psaB*	0.18	21	$1.9\ e^{-2}$
ARTHROv5_50157|psaL (PS I reaction center subunit XI)	*psaL*	0.04	20	$4.3\ e^{-3}$
Gas vesicle related proteins				
ARTHROv5_30356|gvpV (Gas vesicle protein GvpV)	gvpV	0.59	2	$3.4\ e^{-2}$
ARTHROv5_12033|gvpC (Gas vesicle protein GvpC1)	gvpC	0.07	38	$2.0\ e^{-2}$

* Only statistically relevant (p value < 0.05, number of peptides > 1 and fold change ≥1.5 or ≤0.66) results reported here.
** Samples collected post D40 and pre D40 have been respectively classified as late and early stage for scoring purpose. PS I: Photosystem I.

duration' on the photosynthetic cells. However, these studies had been limited to evaluation of pattern of 'growth phase related' secondary metabolite secretion in batch cultures (Ribalet et al., 2007; Loftus and Johnson, 2017), which effectively translated to N depletion related changes rather than the culture run duration related changes. Thus this phenomenon of PBR "aging" is an interesting point of scientific deliberation and should be subjected to detailed future studies, especially in context of MELiSSA loop wherein the cyanobacterium is foreseen to be used for food and O_2 production for manned space missions lasting over years.

The ability of *Arthrospira* sp. to assimilate NH_4^+ without any significant effect on the overall biomass productivity (vs NO_3^-), provides strong opportunities for using NH_4^+ salts for commercial *Arthrospira* sp. production. NH_4^+ fed (8.5 mM) biomass returned 20–30% higher pigments and proteins yields compared to the respective yields reported for the wild-type strain (under N replete conditions). Though the use of a PBR could increase the initial capital and input costs, but the proposed cultivation approach of a continuous PBR and using the light-transfer model for process design, could help in increasing the profitability of the commercial setup. Even though better yields were observed, the 'PBR run duration' based cell-clumping and aggregation could create problems for long duration commercial runs and thus should be to subjected to further scientific deliberation.

4. Conclusions

Unlike previous literature reports, the cultivation approach adopted in this study, demonstrated the possibility of using ammonium salts for commercial *Arthrospira* sp. cultivation, without compromising on biomass productivity. Biochemical and proteomic profiling of cyanobacterial biomass under continuous conditions, highlighted the reasons for the difference in productivities under ammonium and nitrate regimes. These results provide basis for use of ammonium rich wastewater for cyanobacterial cultivation. High pigment, lipid and polysaccharide yields obtained under ammonium feeding regime, illustrated that the presented cultivation approach could be explored for profitable pigments, bioplastics and biofuel production, by reducing dependence on expensive nitrate salts.

Conflict of interest

The authors hereby declare that they do not have any conflict of interests.

Acknowledgements

The authors acknowledge the BELSPO, European Space Agency and University of Mons, Belgium, for providing financial support and funding. This work was also supported by the Belgian Fund for Scientific Research (F.R.S-FNRS). The authors would also like to thank Expert Group for Molecular and Cellular Biology SCK•CEN, Belgium for generously providing Arthrospira sp. PCC 8005 culture.

Appendix A. Supplementary data

Supplementary data associated with this article can be found, in the online version, at https://doi.org/10.1016/j.biortech.2018.07.062.

References

Allen, M.M., Yuen, C., Medeiros, L., Zizlsperger, N., Farooq, M., Kolodny, N.H., 2005. Effects of light and chloramphenicol stress on incorporation of nitrogen into cyanophycin in Synechocystis sp. strain PCC 6308. Biochim. Biophys. Acta. 1725, 241–246.

Baunillo, K.E., Tan, R.S., Barros, H.R., Luque, R., 2012. Investigations on microalgal oil production from *Arthrospira platensis*: towards more sustainable biodiesel production. RSC Adv. 2, 11267–11272.

Bhatnagar, M., Parwani, L., Sharma, V., Ganguly, J., Bhatnagar, A., 2014. Exopolymers from Tolypothrix tenuis and three Anabaena sp. (Cyanobacteriaceae) as novel blood clotting agents for wound management. Carbohydr. Polym. 99, 692–699.

Carvalho, J.C.M., Francisco, F.R., Almeida, K.A., Sato, S., Converti, A., 2004. Cultivation of *Arthrospira (Spirulina) Platensis* (Cyanophyceae) by fed-batch addition of ammonium chloride at exponentially increasing feeding rates. J. Phycol. 40, 589–597.

Chioccioli, M., Hankamer, B., Ross, I.L., 2014. Flow cytometry pulse width data enables rapid and sensitive estimation of biomass dry weight in the microalgae *Chlamydomonas reinhardtii* and *Chlorella vulgaris*. PLoS One. 9, e97269.

Cogne, G., Lehmann, B., Dussap, C.G., Gros, J.B., 2003. Uptake of macrominerals and trace elements by the cyanobacterium *Spirulina platensis* (Arthrospira platensis PCC 8005) under photoautotrophic conditions: culture medium optimization. Biotechnol. Bioeng. 81, 588–593.

Collos, Y., Harrison, P.J., 2014. Acclimation and toxicity of high ammonium concentrations to unicellular algae. Mar. Pollut. Bull. 80, 8–23.

Cornet, J.F., Dussap, C.G., Dubertret, G., 1992. A structured model for simulation of cultures of the cyanobacterium *Spirulina platensis* in photobioreactors: I. Coupling between light transfer and growth kinetics. Biotechnol. Bioeng. 40, 817–825.

Cornet, J.F., Dussap, C.G., Gros, J.B., Binois, C., Lasseur, C., 1995. A simplified monodimensional approach for modeling coupling between radiant light transfer and growth kinetics in photobioreactors. Chem. Eng. Sci. 50, 1489–1500.

Cornet, J.F., Dussap, C.G., 2009. A simple and reliable formula for assessment of maximum volumetric productivities in photobioreactors. Biotechnol. Prog. 25, 424–435.

Dai, G., Deblois, C.P., Liu, S., Juneau, P., Qiu, B., 2008. Differential sensitivity of five cyanobacterial strains to ammonium toxicity and its inhibitory mechanism on the photosynthesis of rice-field cyanobacterium Ge-Xian-Mi (Nostoc). Aquat. Toxicol. 89, 113–121.

Depraetere, O., Pierre, G., Deschoenmaeker, F., Badri, H., Foubert, I., Leys, N., Markou, G., Wattiez, R., Michaud, P., Muylaert, K., 2015. Harvesting carbohydrate-rich *Arthrospira platensis* by spontaneous settling. Bioresour. Technol. 180, 16–21.

Deschoenmaeker, F., Facchini, R., Badri, H., Leroy, B., Zhang, C.C., Wattiez, R., 2014. Proteomic and cellular views of *Arthrospira* sp. PCC 8005 adaptation to nitrogen depletion. Microbiology 160, 1224–1236.

Deschoenmaeker, F., Bayon-Vicente, G., Sachdeva, N., Depraetere, O., Pino, J.C.C., Leroy, B., Muylaert, K., Wattiez, R., 2017. Impact of different nitrogen sources on the growth of Arthrospira sp. PCC 8005 under batch and continuous cultivation – a biochemical, transcriptomic and proteomic profile. Bioresour. Technol. 237, 78–88.

Ivančič, I., Degobbis, D., 1984. An optimal manual procedure for ammonia analysis in natural waters by the indophenol blue method. Water Res. 18, 1143–1147.

Jiang, L., Pei, H., Hu, W., Ji, Y., Han, L., Ma, G., 2015. The feasibility of using complex wastewater from a monosodium glutamate factory to cultivate *Spirulina subsalsa* and accumulate biochemical composition. Bioresour. Technol. 180, 304–310.

Leema, J.T., Kirubagaran, R., Vinithkumar, N.V., Dheenan, P.S., Karthikayulu, S., 2010. High value pigment production from Arthrospira (Spirulina) platensis cultures in seawater. Bioresour. Technol. 101, 9221–9227.

Loftus, S.E., Johnson, Z.I., 2017. Cross-study analysis of factors affecting algae cultivation in recycled medium for biofuel production. Algal Res. 24, 154–166.

Markou, G., Vandamme, D., Muylaert, K., 2014. Ammonia inhibition on *Arthrospira platensis* in relation to the initial biomass density and pH. Bioresour. Technol. 166, 259–265.

Markou, G., 2015. Fed-batch cultivation of Arthrospira and Chlorella in ammonia-rich wastewater: optimization of nutrient removal and biomass production. Bioresour. Technol. 193, 35–41.

Markou, G., Depraetere, O., Muylaert, K., 2016. Effect of ammonia on photosynthetic activity of *Arthrospira* and *Chlorella*: a study on chlorophyll fluorescence and electron transport. Algal Res. 16, 449–457.

Oppermann-Sanio, F.B., Steinbüchel, A., 2002. Occurance, functions and biosynthesis of polyamides in microorganisms and biotechnological production. Naturwissenschaften 89, 11–22.

Patel, R.K., Dodia, M.S., Joshi, R.H., Singh, S.P., 2006. Purification and characterization of alkaline protease from a newly isolated haloalkaliphilic *Bacillus sp*. Process Biochem. 41, 2002–2009.

Persistence Market Research, 2017. Global Market Study on Spirulina: Powder Product Form Segment Anticipated to Dominate the Global Market in Terms of both Value and Volume During 2016–2026. Persistence Market Research Food Innovation Industry Report Code: MRREP14431. Retrieved on 14th November, 2017; from https://www.persistencemarketresearch.com/market-research/spirulina-market.asp.

Ribalet, F., Wichard, T., Pohnert, G., Ianora, A., Miralto, A., Casotti, R., 2007. Age and nutrient limitation enhance polyunsaturated aldehyde production in marine diatoms. Phytochemistry 68, 2059–2067.

Rodrigues, M.S., Ferreira, L.S., Converti, A., Sato, S., Carvalho, J.C.M., 2010. Fed-batch cultivation of *Arthrospira* (Spirulina) *platensis*: Potassium nitrate and ammonium chloride as simultaneous nitrogen sources. Bioresour. Technol. 101, 4491–4498.

Roose, J.L., Kashino, Y., Pakrasi, H.B., 2007. The PsbQ protein defines cyanobacterial Photosystem II complexes with highest activity and stability. PNAS 104, 2548–2553.

Sachdeva, N., Kumar, G.D., Gupta, R.P., Mathur, A.S., Manikandan, B., Basu, B., Tuli, D.K., 2016a. Kinetic modeling of growth and lipid body induction in *Chlorella pyrenoidosa* under heterotrophic conditions. Bioresour. Technol. 218, 934–943.

Sachdeva, N., Gupta, R.P., Mathur, A.S., Tuli, D.K., 2016b. Enhanced lipid production in thermo-tolerant mutants of *Chlorella pyrenoidosa* NCIM 2738. Bioresour. Technol. 221, 576–587.

Sassano, C.E.N., Gioielli, L.A., Ferreira, L.S., Rodrigues, M.S., Sato, S., Converti, A., Carvalho, J.C.M., 2010. Evaluation of the composition of continuously-cultivated

Arthrospira (Spirulina) platensis using ammonium chloride as nitrogen source. Biomass Bioenergy 34, 1732–1738.
Sesták, Z., 1971. Determination of chlorophylls a and b. In: Plant Photosynthetic Production: Manual of Methods. Dr. W. Junk NV, The Hague, The Netherlands, pp. 672–701.
Shirazi, H.M., Karimi-Sabet, J., Ghotbi, C., 2017. Biodiesel production from *Spirulina* microlagae feedstock using direct transesterification near supercritical methanol condition. Bioresour. Technol. 239, 378–386.
Smetana, S., Sandmann, M., Rohn, S., Pleissner, D., Heinz, V., 2017. Autotrophic and heterotrophic microalgae and cyanobacteria cultivation for food and feed: life cycle assessment. Bioresour. Technol. 245, 162–170.
Spolaore, P., Joannis-Cassan, C., Duran, E., Isambert, A., 2006. Commercial applications of microalgae. J. Biosci. Bioeng. 101, 87–96.
Trebitsh, T., Danon, A., 2001. Translation of chloroplast *psb*A mRNA is regulated by signals initiated by both photosystems II and I. PNAS 98, 12289–12294.
Xu, H., Vavilin, D., Vermass, W., 2001. Chlorophyll *b* can serve as the major pigment in functional photosystem II complexes of cyanobacteria. PNAS 98, 14168–14173.
Zeller, M.A., Hunt, R., Jones, A., Sharma, S., 2013. Bioplastics and their thermoplastic blends from *Spirulina* and *Chlorella* microalgae. J. Appl. Polym. Sci. 130, 3263–3275.
Zhou, W., Li, Y., Gao, Y., Zhao, H., 2017. Nutrients removal and recovery from saline wastewater by *Spirulina platensis*. Bioresour. Technol. 245, 10–17.